Available online at www.sciencedirect.com

ScienceDirect

Procedia CIRP 75 (2018) 226–231

www.elsevier.com/locate/procedia

15th CIRP Conference on Computer Aided Tolerancing – CIRP CAT 2018

Consideration of Working Conditions in Assembly Tolerance Analysis

Liu Ting[b], Zhu Zuowei[c], Cao Yanlong[a,b]*, Nabil Anwer [c], Yang Jiangxin[b]

[a]State Key Laboratory of Fluid Power and Mechatronic Systems, School of Mechanical Engineering, Zhejiang University, Hangzhou, 310027, China

[b]Key Laboratory of Advanced Manufacturing Technology of Zhejiang Province, School of Mechanical Engineering, Zhejiang University

[c] LURPA, ENS Paris-Saclay, Univ. Paris-Sud, Université Paris-Saclay, 94235 Cachan, France

* Corresponding author. Tel.: +86-571-87953198; fax: +86-571-87951145. *E-mail address:* sdcaoyl@zju.edu.cn

Abstract

Mechanical deviations induced by working conditions are always ignored in assembly analysis due to the rigid body hypothesis of parts. This paper presents a study of the deviations resulting from the actual working conditions. Finite element analysis (FEA) is conducted to simulate the deviations occurring in assemblies, in which the point-cloud geometry representation of deformed parts is adopted to enable the calculation of small displacements by means of relative positioning. The simulated deviations are incorporated in manufacturing deviations to determine the functional requirements based on Jacobian-torsor model. The approach is finally illustrated by a practical example.

Peer-review under responsibility of the Scientific Committee of the 15th CIRP Conference on Computer Aided Tolerancing - CIRP CAT 2018.

Keywords: working condition, tolerance analysis, Jacobian-torsor

1. Introduction

Tolerance analysis is performed in manufacturing to predict the quality of an assembly when the tolerances have been assigned to its components. A proper analysis result can be the guidance for industries to optimize parameters in design. The dimensional and geometric variations of each part in assembly have to be limited by tolerances to ensure not only a standardized production but also a conformation to the functional requirements assigned on the whole assembly. To calculate the accumulated error resulting from a stack-up of dimensions and tolerances, two aspects have to be paid attention to, namely tolerance representation which determines the meaning of the applied tolerance specifications, and tolerance propagation which is the process for determining the cumulative variation possibilities among two or more features. In the literature, a variety of models are proposed to carry out a tolerance analysis of an assembly, i.e., Variation model [1], TTRS model [2], Matrix model [3], Vector loop [4], Jacobian model [5], Torsor model [6], Jacobian-tosor model [7], GapSpace [8], T-Map model [9], Deviation domain [10], Polytopes [11] and Skin model shapes [12], among which Jacobian model is well-known for tolerance propagation from part to part in assembly, and the Torsor model is an easy-to-use model to represent the constraints of tolerances by screw parameters. In order to overcome the disadvantages of the Torsor model in representing the deviation propagation, the Jacobian model has been integrated into it, making the Unified Jacobian-torsor, which is quite suitable for complex assemblies containing a large number of joints and geometric tolerances.

A hypothesis is normally made on these models that the different parts are modelled as infinitely rigid solids. However, in actual working conditions, many factors such as temperature, force, gravity, wear and friction may result in a difference in dimension, angle and shape. Taking the turbine as an example [13], when the turbine is operating, a flux of hot gases (about 1000°C) is sprayed from the combustion chamber. Under the high temperature, clearances and dimensions of geometric features are obviously different from their static condition, thus reducing the system reliability. S. Benichou et al. [14] integrate thermal dilatation in function tolerancing. Stuppy adds deformation deviation in a crank mechanism [15]. G.

2212-8271 © 2018 The Authors. Published by Elsevier B.V.
Peer-review under responsibility of the Scientific Committee of the 15th CIRP Conference on Computer Aided Tolerancing - CIRP CAT 2018.
10.1016/j.procir.2018.02.003

Jayaprakash et al. [16] consider the effect of thermal and inertia on optimal tolerance value of components in design. Walter et al. account for deviations from manufacturing discrepancies or operation-dependent deviations into the simulation analysis [17]. Junkang Guo proposes a model to equivalently represent the elastic mating surfaces with geometric variation and deformation [18]. Moreover, Corrado presents a comprehensive study of tolerance analysis for rigid part with manufacturing signature and operating conditions [19].

FEA simulation, as a virtual tool, is commonly used to obtain the actual deformations in a designed mechanical part caused by all of its operational loads. Typical FEA software includes ANSYS Mechanical, ABAQUS, Romax, I-DEAS, CAST3M, and SIMULIA. The deformed shapes represented with a set of points are associated by the least squares method and the variation error is evaluated as the transform matrix between the associated surface and the nominal surface [20, 21]. Alternatively, analogous analysis is conducted on the inputs and outputs to derive the mathematical relation between variations and loads [22]. In this paper, an approach is proposed to conduct deviation propagation and accumulated error calculation with consideration of both manufacturing error and deformation error in assembly based on the Jacobian–torsor model. Finite element analysis is performed on nominal model and displacement of every point of parts under the effect of working condition is obtained. The relative positioning of this deformed geometry and its corresponding nominal model gives the small variation torsor which is then integrated into the Jacobian–torsor model to obtain the functional requirement.

The reminder of this paper is organized as follows. Section 2 provides a review of the Jacobian–torsor model, and the solutions of obtaining deformation variation as well as integrating it into the unified Jacobian–torsor model are presented. Section 3 demonstrates this method by a case study. Section 4 draws the conclusion.

2. Tolerance analysis based on Jacobian-torsor

2.1. Jacobian-torsor model

In the assembly process, the accumulated error of functional requirement is determined by propagation and stack-up of all deviations. The unified Jacobian-torsor model introduced by Desrochers et al [7] is a method that combines two models, i.e., the Jacobian model and the Torsor model which are effective for tolerance propagation and tolerance representation respectively.

The small displacement torsor (SDT) model uses screw parameters including three translational vectors and three rotational vectors to represent small displacements of a feature within its tolerance zone. Jacobian matrix is used to map all SDT from their local origin to the point of interest. Once the constraints of typical features are established to transform different forms of tolerances into variable domain of SDT, the final error can be achieved through error propagation process by the Jacobian matrix. Therefore, Jacobian–torsor model can be expressed as follows:

$$[FR]=[J][FE] \tag{1}$$

where the functional requirement (play, gap, clearance) represented by [FR] is the translational and rotational vectors of general assembly. [FE] is the small displacement torsor related to each function element. [J] is a Jacobian matrix expressing a geometrical relation between a [FR] vector and corresponding [FE] vector which can be expressed by:

$$[J]_{FEi}=\begin{bmatrix} \left[R_0^i\right]_{3\times3}\cdot\left[R_{PT_i}^i\right]_{3\times3} & \cdots & \left[W_i^n\right]_{3\times3}\left(\left[R_0^i\right]_{3\times3}\cdot\left[R_{PT_i}^i\right]_{3\times3}\right) \\ \vdots & \ddots & \vdots \\ [0]_{3\times3} & \cdots & \left[R_0^i\right]_{3\times3}\cdot\left[R_{PT_i}^i\right]_{3\times3} \end{bmatrix}_{6\times6} \tag{2}$$

where $\left[R_0^i\right]=[C_{1i}C_{2i}C_{3i}]$ represents the local orientation of ith frame with respect to *0*th frame that is the global reference system; $[R_{PTi}]=[C_1C_2C_3]_{PTi}$, $C_1C_2C_3$ represents the directional change of tolerance with respect to the three coordinate axes of frame i;. $[w_i^n]=\begin{bmatrix} 0 & -dz_i^n & dy_i^n \\ dz_i^n & 0 & -dx_i^n \\ -dy_i^n & dx_i^n & 0 \end{bmatrix}$ is a skew-symmetric matrix, indicating the positional changes for frame n with respect to frame i . In w_i^n , $dx_i^n=dx_n-dx_i, dy_i^n=dy_n-dy_i$, and $dz_i^n=dz_n-dz_i$.

The functional requirement [FR] at assembly level can be derived from above equations.

2.2. Integration of deformation

During a practical working situation, the multiple fields that are applied to single parts or assembly, such as temperature filed and force field, result in geometric errors and dimensional changes in size, direction and magnitude in spatial six degrees of freedom. Taking the bourdon tube in Fig.1 as an example, a bending load is imposed on it during its working condition. As a consequence, the whole bourdon tube tilts to the side of the load. The larger the bending load, the bigger the bending deflection. The point clouds of the deformed tube shape can be obtained through FEA simulation that takes all the effects of working conditions into consideration.

The small displacement variations induced from deformations can be regarded as a relative positioning problem between deformed surfaces and their corresponding nominal surfaces (see Fig.2). The relative positioning of two surfaces is solved based on an optimization problem with "best-fit" requirement. The implemented algorithm aims at minimizing the distances between any point on one surface and the corresponding closest point of the other surface by iteratively adjusting the transformation matrix. The variational torsor (Δ) due to the deformation can be defined by six components, including three translational components represented as Δu, Δv and Δw and three rotational components represented as Δα, Δβ and Δγ, as seen in Eq.(3).

$$\Delta=[\Delta u;\Delta v;\Delta w;\Delta\alpha;\Delta\beta;\Delta\gamma] \tag{3}$$

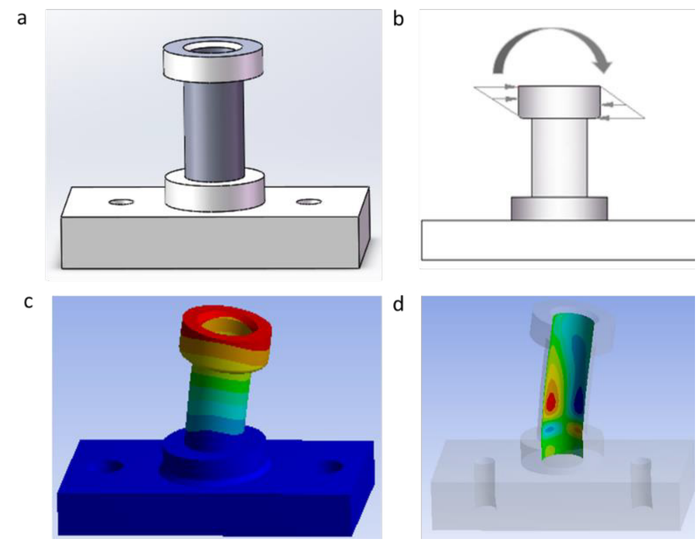

Fig.1. (a) Bourdon tube model; (b) Load diagram; (c) Total deformation of part. (d) Internal deformed surface

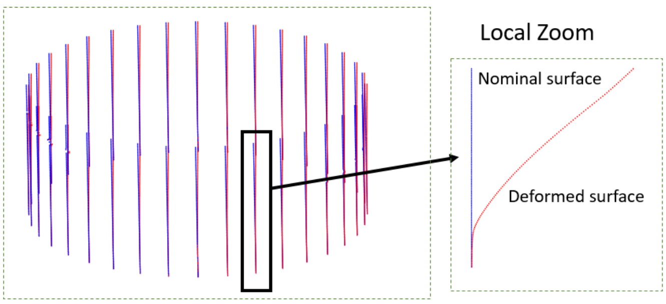

Fig.2. Deformed and nominal surface of Fig.1(d).

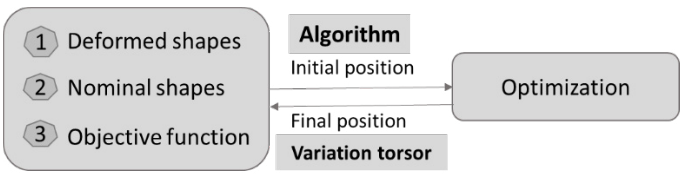

Fig.3 The relative positioning framework

The deformed surface in Fig.1d is taken as an example to illustrate the process of obtaining variational torsor for deformed part in Fig.1c based on relative positioning method. The framework of the method is shown in Fig.3. The whole process can be divided into three steps:
Step1: Search for the corresponding point pairs of two surfaces. Based on Delaunay triangulation, for every point of the deformed shape A, the corresponding point on its nominal feature B is determined as the point that has the minimal Euclidean distance:

$$B_{A_i} = B_j ; j = \arg\min \left\| A_i - B_j \right\| \tag{4}$$

where B_{A_i} means the corresponding point in feature B for A_i, as depicted in Fig.4.

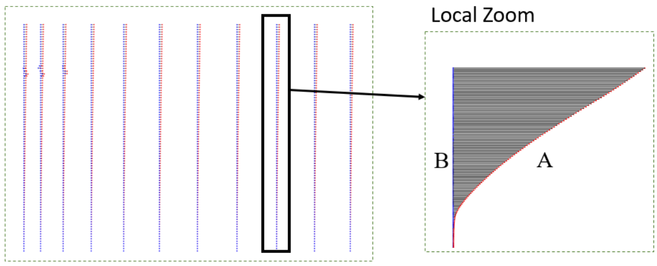

Fig.4. Determination of point correspondences

Step2: Define objective functions. The objective function is defined as the minimization of the squared sum of Euclidean distances between all points of deformed surface and their correspondences in the nominal surface, as shown in Eq.(5):

$$\min f = \sum_{i=1}^{N} \left\| T_r \cdot A_i + T_t - B_{A_i} \right\|^2 \tag{5}$$

where N represents the number of points on the deformed surface. T_r =[Δα; Δβ; Δγ] is the variational rotation vector and $T_t = [\Delta u; \Delta v; \Delta w]$ is the variational translation vector.
Step3: "Best-fit" solution. An adequate algorithm has to be chosen in this step to return the optimal variational torsor. This can be performed by minimizing the objective function in Step 2 employing an active set, sequential quadratic programming (SQP) or iHLRF algorithms [23].

The obtained deformation torsor brings about small changes to the local coordinate system associated with the part. As a consequence, functional element FE in Eq. (1) varies as well. Then we have parameters in Eq. (2) as:

$$R_0^{i'} = R_0^{i} \left[C_{xi} \right] \left[C_{yi} \right] \left[C_{zi} \right] \tag{6}$$

where $[C_{xi}]$ is a transition matrix that rotates Δα around the x axis on frame i. It can be computed as follows.

$$\left[C_{xi} \right] = \begin{bmatrix} 1 & 0 & 0 \\ 0 & \cos\Delta\alpha & -\sin\Delta\alpha \\ 0 & \sin\Delta\alpha & \cos\Delta\alpha \end{bmatrix} \tag{7}$$

In the same way, we can get $[C_{yi}]$ and $[C_{zi}]$ that separately represent transition matrices around the y and z axis on frame i with angles Δβ and Δγ.

$$\left[C_{yi} \right] = \begin{bmatrix} \cos\Delta\beta & 0 & \sin\Delta\beta \\ 0 & 1 & 0 \\ \sin\Delta\beta & 0 & \cos\Delta\beta \end{bmatrix} \qquad \left[C_{zi} \right] = \begin{bmatrix} \cos\Delta\gamma & -\sin\Delta\gamma & 0 \\ \sin\Delta\gamma & \cos\Delta\gamma & 0 \\ 0 & 0 & 1 \end{bmatrix} \tag{8}$$

Due to the fact that $R_{PTi'}$describes the directional change of tolerance with respect to the frame i' in working condition, it can be deduced as:

$$\left[R_{PTi'} \right]^{-1} = \left[R_{PTi} \right]^{-1} \cdot \left[C_{xi} \right] \cdot \left[C_{yi} \right] \cdot \left[C_{zi} \right] \tag{9}$$

Considering the translational variations, the dx_i^n, dy_i^n and dz_i^n can be deduced as:

$$\begin{aligned} dx_{i'}^{n'} &= dx_{n'} - dx_{i'} = dx_i^n + (\Delta u_n - \Delta u_i) \\ dy_{i'}^{n'} &= dy_{n'} - dy_{i'} = dy_i^n + (\Delta v_n - \Delta v_i) \\ dz_{i'}^{n'} &= dz_{n'} - dz_{i'} = dz_i^n + (\Delta w_n - \Delta w_i) \end{aligned} \tag{10}$$

Substituting the above three parameters in w_i^n, we obtain $w_{i'}^{n'}$. Then combining Eqs. (6-10), the Jacobian matrix can be defined as:

$$[J]_{FEi'} = [J]_0^{i'} = \begin{bmatrix} [R_0^i]_{3\times3}\,[R_{PT_i}^i]_{3\times3} & \cdots & [W_{i'}^{n'}]_{3\times3}\left([R_0^i]_{3\times3}\cdot[R_{PT_i}^i]_{3\times3}\right) \\ \vdots & \ddots & \vdots \\ [0]_{3\times3} & \cdots & [R_0^i]_{3\times3}\cdot[R_{PT_i}^i]_{3\times3} \end{bmatrix}_{6\times6} \tag{11}$$

Besides, [FE] can be rewritten as:

$$[FE]_{FEi'} = \begin{bmatrix} [R_{PTi'}]^{-1}\cdot T_{FEi} \\ [R_{PTi'}]^{-1}\cdot R_{FEi} \end{bmatrix} \tag{12}$$

where T_{FEi} and R_{FEi} are the translational and rotational torsor components originated from applied tolerances.

Once we have $[J]_{FEi'}$ and $[FE]_{FEi'}$, the functional requirement $[FR]'$ can be derived. The framework proposed to analyse the accumulated error for functional requirement with consideration of manufacturing error and deformation error in working condition is shown in Fig.5. For the first step, we consider the functional requirement due to manufacturing error, i.e., dimensional and geometric deviations. Since the key point is to obtain the variation torsor resulting from deformation, therefore, in the second step, the simulation is conducted and the deformations are retrived from the simulation result. This procedure includes the import of CAD models into FEA software, the definition of property, mesh and constrains, and the export of deformed point clouds and nominal point clouds for features. Then relative positioning approach is applied to yield the variational torsor. Finally, the components in rotation and translation will be used to modify the parameters in the first step.

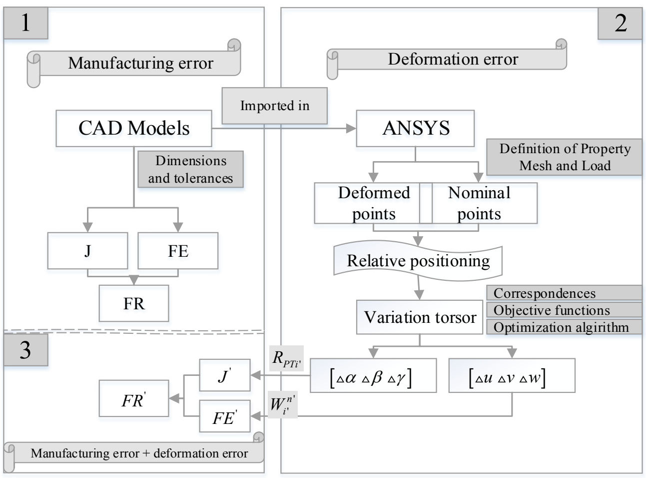

Fig. 5. Procedures to calculate accumulated error for assembly

3. Case study

We shall now apply the proposed method for accumulated error calculation based on a simple mechanism, as illustrated in Fig.6. This assembly is made up of two parts: Support and Probe. The tolerances and dimensions are specified in Fig.7. The reference frames are in the middle of the tolerance or contact uncertainty zone. Then a connection graph is constructed to establish the dimensional chains, as depicted in Fig.8.The kinematic chain contains two internal pair (FE0,FE1) and (FE2,FE3), as well as one contact pair (FE1,FE2). The functional condition FR implies the control of the relative position between the end of Probe, which is accumulated by all tolerances of two parts and one joint, and the surface of the datum A.

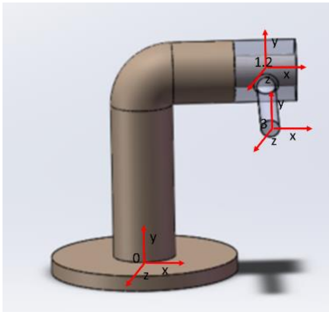

Fig.6. Example mechanism

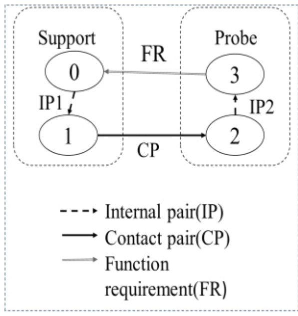

Fig.8. Connection graph

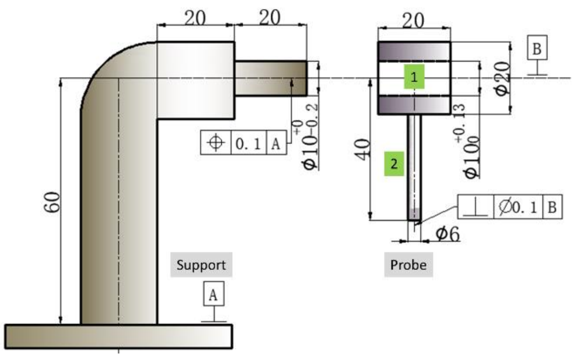

Fig.7. Detailed drawing of assembly

Table 1 summarizes the Jacobian matrices and torsors associated to the respective function element pairs identified in Fig. 8, and according to the procedures described in Section 2.1. The FR_0 taking only manufacturing error into account can be expressed in Eq. (13).

Table 1. Jacobian and torsor details.

Pair	Jacobian	Torsor
IP1	$\begin{bmatrix} 1&0&0&0&-40&0 \\ 0&1&0&40&0&0 \\ 0&0&1&0&0&0 \\ 0&0&0&1&0&0 \\ 0&0&0&0&1&0 \\ 0&0&0&0&0&1 \end{bmatrix}$	$\begin{bmatrix} (0,0) \\ [-0.1/2,+0.1/2] \\ [-0.1/2,+0.1/2] \\ [0,0] \\ [-0.1/20,+0.1/20] \\ [-0.1/20,+0.1/20] \end{bmatrix}$
CP	$\begin{bmatrix} 1&0&0&0&-40&0 \\ 0&1&0&40&0&0 \\ 0&0&1&0&0&0 \\ 0&0&0&1&0&0 \\ 0&0&0&0&1&0 \\ 0&0&0&0&0&1 \end{bmatrix}$	$\begin{bmatrix} (0,0) \\ [-0.33/2,+0.33/2] \\ [-0.33/2,+0.33/2] \\ [0,0] \\ [-0.33/20,+0.33/20] \\ [-0.33/20,+0.33/20] \end{bmatrix}$

IP2	$\begin{bmatrix} 1 & 0 & 0 & 0 & 0 & 0 \\ 0 & 1 & 0 & 0 & 0 & 0 \\ 0 & 0 & 1 & 0 & 0 & 0 \\ 0 & 0 & 0 & 1 & 0 & 0 \\ 0 & 0 & 0 & 0 & 1 & 0 \\ 0 & 0 & 0 & 0 & 0 & 1 \end{bmatrix}$	$\begin{bmatrix} [-0.1/2,+0.1/2] \\ [-0.1/2,+0.1/2] \\ [0,0] \\ [-0.1/30,+0.1/30] \\ [-0.1/30,+0.1/30] \\ [0,0] \end{bmatrix}$

$$FR_0 = \left[[J]_{FE1}[J]_{FE2}[J]_{FE3}\right] \begin{bmatrix} [-0.8100,+0.8100] \\ [-0.2650,+0.2650] \\ [-0.2150,+0.2150] \\ [-0.0005,+0.0005] \\ [-0.0265,+0.0265] \\ [-0.0215,+0.0215] \end{bmatrix} \tag{13}$$

An FEA simulation of the assembly is carried out on the nominal part model. The material properties are defined, together with a load that specifies a 100N force at the end of the Probe in $-y$ direction and a fixed constraint on Support. The geometry and displacement of surfaces that are deformed by the force are simulated in ANSYS software (see Fig.9). The actual position and nominal position for each point of surfaces can be exported as their Cartesian coordinates respectively.

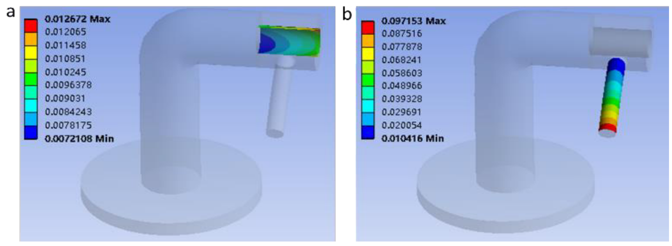

Fig.9. (a) FEA for Support; (b) FEA for Probe. Note that the deformations in figures are expressed in millimeter (mm).

Taking the cylindrical surface in Fig.9b as an example, the point clouds for deformed and nominal surfaces can be derived in Fig.10. Assuming that $\mathrm{A} = \{\mathrm{A}_i \in \mathrm{R}^3, i = 1,2 \dots\dots, \mathrm{N}\}$ and $\mathrm{B} = \{\mathrm{B}_i \in \mathrm{R}^3, i = 1,2 \dots\dots, \mathrm{N}\}$ are these two point clouds, where N represents the number of meshed nodes generated in ANSYS, the variation from A to B can be expressed as:

$$B = T_r \cdot A + T_t \tag{14}$$

where T_r is the rotational components and T_t is the translational components.

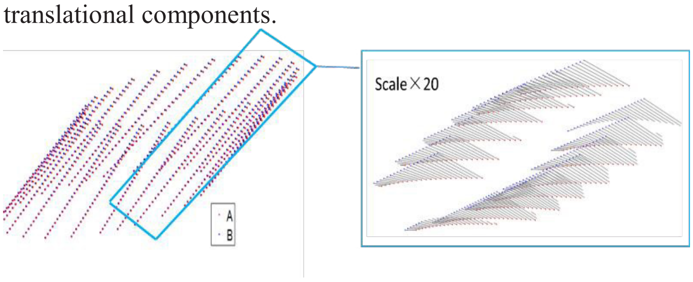

Fig.10. Correspondence for Probe.

Following the three steps of relative positioning, corresponding points in nominal surface are identified (see Fig.10), and the objective function is defined (see Eq. (15)) and minimized to give an optimal variational torsor.

$$\min_{T_r,T_t} f\left(T_r \cdot A + T_t, \mathrm{B}\right) \tag{15}$$

Subject to $lb \leq T_r, T_t \leq ub$

In Eq.(15), lb and ub are vectors of the lower and higher limit defining the variations in six degrees of freedom and can be represented by $lb = [-1,-1,-1,-\mathrm{inf},-\mathrm{inf},-\mathrm{inf}]; ub = [1,1,1,\mathrm{inf},\mathrm{inf},\mathrm{inf}]$.

Several algorithms can be used to solve this optimization problem. In this paper, sequential quadratic programming (SQP) is adopted and the obtained solutions of deformation variations in Fig. 9(a-b) are listed in Table 2.

Table2 Torsor variations result from deformation

Pair	IP1	IP2
Variations(Δ)	$\begin{bmatrix} -0.0016 \\ -0.0163 \\ -3.7425E-04 \\ -2.4997E-04 \\ -1.3584E-07 \\ 1.8849E-04 \end{bmatrix}$	$\begin{bmatrix} -0.0015 \\ -0.2886 \\ 0.0377 \\ -0.0030 \\ -7.1821E-07 \\ 1.9409E-04 \end{bmatrix}$

It should be noted that the translational variations of IP1 and IP3 have influence on parameters w_i^n and then affect the Jacobian matrices. According to Eq. (12), functional element vectors should be modified due to the effect of rotational variations on reference frames. The functional requirement FR_1considering manufacturing error and deformation error can be therefore computed using Eq. (1), the result is compared with FR_0 that ignores the deformation in working condition. The comparison result shows that the limit of x-translation increases from ±0.8100 mm to ±0.8169 mm while the limits of y and z-translation drop from ±0.2650 mm and ±0.2150mm to ±0.2649mm and ±0.2148mm, respectively. It is obvious that the variations in y and z are small compared to changes in x-axis. The deformation makes no difference in accumulated rotation error. For better illustration of the method, we make another experiment by imposing a 200 N force on Probe in $-y$ direction. The result of functional requirement is shown in Eq. (17), the tendency of variation is consistent with that of FR_1in Eq. (16), and the deviation of FR_2 from FR_0 is nearly twice as that of FR_1 from FR_0. The benefit of this solution for tolerance analysis is that actual working condition is considered and integrated into the Unified Jacobian-Torsor model to increase the accuracy and reliability of the results.

$$FR_1 = \begin{bmatrix} [-0.8169,+0.8169] \\ [-0.2649,+0.2649] \\ [-0.2148,+0.2148] \\ [-0.0050,+0.0050] \\ [-0.0265,+0.0265] \\ [-0.0215,+0.0215] \end{bmatrix} \tag{16}$$

$$FR_2 = \begin{bmatrix} [-0.8239,+0.8239] \\ [-0.2648,+0.2648] \\ [-0.2146,+0.2146] \\ [-0.0050,+0.0050] \\ [-0.0265,+0.0265] \\ [-0.0215,+0.0215] \end{bmatrix} \tag{17}$$

4. Conclusion

Induced by manufacturing variations and deformation variations, errors can be accumulated from part to part throughout the assembly. However, the deformation in working condition is normally neglected in most models in calculation of variation propagation and tolerance analysis based on the rigid body assumption. In this paper, a solution has been proposed integrating working condition into the Jacbian-torsor model for tolerance analysis. Using the FEA, deformation of parts can be simulated. The relative positioning of deformed shapes and nominal shapes enable the calculation of variation torsors. An industrial application of an example mechanism with operational force is provided as a demonstration. By taking the force-induced deformation into consideration, the final calculated deviation, especially x-translation of this assembly is more than that calculated by the traditional Jacobian-torsor model. In addition, the larger the imposed force, the bigger the final deviation is. A comparison of the results proves that the proposed method gives a more effective and reliable solution as well as optimized product performance.

The relative positioning method enables the convenient calculation of the variational torsor parameters resulting from actual loads in working condition. Based on this method, the Jacobian-torsor model can be quite suitable for tolerance analysis of mechanisms in special working environments, such as high temperature and high pressure, i.e., combustion engine. It is a supplement of this model that the accuracy and reliability can be largely improved.

This article aims at simulating deformations on nominal CAD model by FEA. It can be possibly extended to operate on toleranced surfaces with manufacturing deviations, such as skin model shapes [12]. Besides, due to the fact that the Jacobian-torsor model currently still has difficulty in the application of over-constrained system, this method mainly focuses on isostatic architecture at present. These work will be further studied and addressed in future research.

Acknowledgements

This research was supported by the National Natural Science Foundation of China (No. 51575484 and U1501248), Science Fund for Creative Research Groups of National Natural Science Foundation of China (No. 51521064) and the China Scholarship Council (CSC).

References

[1] Franciosa P, Gerbino S, Patalano S. Variational modeling and assembly constraints in tolerance analysis of rigid part assemblies: planar and cylindrical features. Int J Adv Manuf Technol 2010;49:239-51.
[2] Liu J, Wilhelm RG. Genetic algorithms for TTRS tolerance analysis. Geometric Product Specification and Verification: Integration of Functionality: Springer; 2003. p. 73-82.
[3] Desrochers A, Rivière A. A matrix approach to the representation of tolerance zones and clearances. Int J Adv Manuf Technol 1997;13:630-6.
[4] Chase KW. Tolerance Analysis of 2-D and 3-D Assemblies (automated method).
[5] Lafond P, Laperriere L. Jacobian-based modeling of dispersions affecting pre-defined functional requirements of mechanical assemblies. in Assembly and Task Planning, 1999 (ISATP '99) Proceedings of the 1999 IEEE International Symposium on. 1999 of Conference.
[6] Bourdet P, Mathieu L, Lartigue C, Ballu A. The concept of the small displacement torsor in metrology. Series on advances in Mathematics for Applied Sciences 1996;40:110-22.
[7] Ghie W, Laperrière L, Desrochers A. A Unified Jacobian-Torsor Model for Analysis in Computer Aided Tolerancing: Springer Netherlands, 2003, p.63-72.
[8] You X. GapSpace multi-dimensional assembly analysis. Dissertations & Theses - Gradworks 2008.
[9] Ameta G, Davidson JK, Shah JJ. Statistical Tolerance Allocation for Tab-Slot Assemblies Utilizing Tolerance-Maps. J Comput Inf Sci Eng 2010;10:237-56.
[10] Giordano M, Samper S, Petit JP. Tolerance analysis and synthesis by means of deviation domains, axi-symmetric cases: Springer Netherlands, 2007, p.85-94.
[11] Homri L, Teissandier D, Ballu A. Tolerancing Analysis by Operations on Polytopes. 2013: 597-604.
[12] Anwer N, Schleich B, Mathieu L, Wartzack S. From solid modelling to skin model shapes: Shifting paradigms in computer-aided tolerancing. CIRP Ann 2014;63:137-40.
[13] Pierre L, Teissandier D, Nadeau JP. Integration of thermomechanical strains into tolerancing analysis. Int J Interact Des Manuf 2009;3:247-63.
[14] Benichou S, Anselmetti B. Thermal dilatation in functional tolerancing. Mech Mach Theory 2011;46:1575-87.
[15] Stuppy J, Meerkamm H. Tolerance analysis of a crank mechanism by taking into account different kinds of deviation. in Proceedings of the 11th CIRP international seminar on computer aided tolerancing. 2009 of Conference.
[16] Govindarajalu J, Karuppan S, Manoharan T. Tolerance design of mechanical assembly using NSGA II and finite element analysis. J Mech Sci Technol 2012;26:3261-8.
[17] Walter M, Breitsprecher T, Gruber G, Wartzack S. Simulation based generation of an initial design taking into account geometric deviations and deformations. in DS 68-10: Proceedings of the 18th International Conference on Engineering Design (ICED 11), Impacting Society through Engineering Design, Vol 10: Design Methods and Tools pt 2, Lyngby/Copenhagen, Denmark, 15-1908 2011. 2011 of Conference.
[18] Guo J, Li B, Liu Z, Hong J, Wu X. Integration of geometric variation and part deformation into variation propagation of 3-D assemblies. Int J Prod Res 2016;54:5708-21.
[19] Corrado A, Polini W. A comprehensive study of tolerance analysis methods for rigid parts with manufacturing signature and operating conditions. J Adv Mech Des Syst 2017;11:JAMDSM0017.
[20] Pierre L, Teissandier D, Nadeau JP. Integration of thermomechanical strains into tolerancing analysis. Int J Interact Des Manuf 2009;3:247-63.
[21] Guo J, Hong J, Yang Z, Wang Y. A tolerance analysis method for rotating machinery. Procedia CIRP 2013; 10: 77-83.
[22] Ghie W, Laperrière L, Desrochers A. Re-Design of Mechanical Assemblies using the Unified Jacobian-Torsor Model for Tolerance Analysis: Springer Netherlands, 1970, p.95-104.
[23] Homri L, Goka E, Levasseur G, Dantan J-Y. Tolerance analysis — Form defects modeling and simulation by modal decomposition and optimization. Comput Aid Des 2017;91:46-59.